

## Cardiac Applications of Positron Emission Tomography

David Mankoff, Ralph G. Nader, and Howard J. Eisen

*University of Pennsylvania School of Medicine, Philadelphia, Pennsylvania*

---

*This is the second in a series of four continuing education articles on positron emission tomography (PET) imaging. After reviewing this article the reader should be able to: (1) understand the clinical considerations for PET imaging of the heart; (2) understand the technical considerations for PET imaging of the heart; and (3) be familiar with the agents used in PET imaging of the heart.*

---

Cardiovascular imaging has traditionally relied on two broad categories of modalities to obtain information about the heart. Functional imaging, which provides information about cardiac function and left ventricular wall motion, is a category that includes contrast angiography, echocardiography, radionuclide angiography and more recently, magnetic resonance imaging (MRI) and ultrafast computed tomography (CT). The second broad category is physiologic imaging, including thallium-201 ( $^{201}\text{Tl}$ ) scintigraphy to assess myocardial perfusion and echocardiography which can provide hemodynamic information noninvasively. Positron emission tomography (PET) is an investigational imaging technique which can provide physiologic and metabolic information noninvasively and may ultimately become an important clinical tool. Prior work has shown that myocardial metabolism, quantitative and qualitative determinations of coronary artery blood flow, myocardial adrenergic innervation and other physiologic parameters can be assessed with PET. The present uses of PET in cardiology as well as its future utility will be reviewed in this article (see Table 1).

### CLINICAL CONSIDERATIONS

At the present time PET is primarily a research tool, though several institutions are using this imaging modality for clinical purposes. Specific types of studies, which will be detailed subsequently, include noninvasive assessment of coronary blood flow, myocardial viability and perturbations in myocardial adrenergic innervation. Coronary artery disease, which is the major killer in the United States, results in marked

limitations in regional coronary blood flow. This can, in turn, cause significant myocardial ischemia or myocardial infarction. Determination of degree of reversible or ischemic myocardial dysfunction, as well as extent of limitation of coronary blood flow in patients with coronary disease can be assessed noninvasively using PET. Therefore, PET plays an important role in cardiovascular research and, ultimately, may play a similar role in clinical care in patients with coronary artery disease. Newer imaging modalities such as those available for measuring myocardial adrenergic innervation may extend the utility of PET to other groups of patients with cardiovascular disease, such as cardiomyopathy or arrhythmias.

### TECHNICAL CONSIDERATIONS

The general technical considerations that apply to PET are reviewed in another article in this series; here we highlight those considerations particular to cardiac PET imaging. Excellent overviews of general PET technical considerations are given (1-4).

#### Patient Positioning

Tomographs designed for body imaging typically have patient openings of 50-65 cm (5) in diameter to assure that all but the largest patients' bodies will fit in the tomograph. The size of the patient part is limited by the need to shield the patient opening (using lead plates) from radiation arising from the patient's body outside the field of view (6-8). Since most cardiac agents widely distribute in the body, the patient opening must be shielded from both the front and the back. This consideration is taken into account by most tomograph designers.

Because the bones in arms strongly attenuate the annihilation photons, if possible, the arms should be placed outside the patient port during imaging. It is therefore important that distance between the outside of the scanner and the active patient port be minimized so that the patient may comfortably place his arms outside of the tomograph; otherwise, the patient is forced to hold his arms in an uncomfortable position above his head during the entire scan. For tomographs with sufficient travel in the patient bed, a "feet-first" position provides comfort for the patient, as well as easy access for physicians and technologists in the event of an emergency.

---

For reprints contact: Howard J. Eisen, MD, Cardiovascular Section, Department of Medicine, Hospital of the University of Pennsylvania, 9 Gates Building, 3400 Spruce St., Philadelphia, PA 19104.

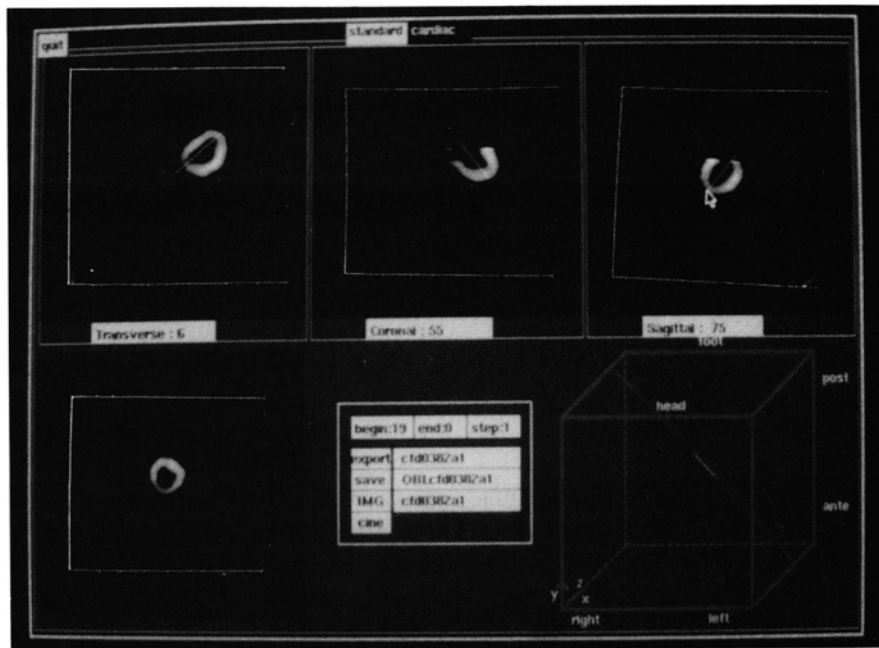


**FIG. 1.** Demonstration of re-slicing into cardiac short axis views. Transverse, coronal and sagittal views are shown on the top line with the base-to-apex axis drawn on each image (lines and pointer). This information is used to determine the cardiac short-axis, and a short-axis view (lower left) is generated from the three-dimensional image data. The illustration in the lower right helps the user identify the three-dimensional orientation of the re-sliced image. (Photo courtesy University of Pennsylvania Nuclear Medicine Physics and Instrument Group and UGM Medical Systems.)

## Exercise Studies

Many cardiac imaging protocols require a comparison of images acquired with the patient in the resting state and exercise state, analogous to the stress-redistribution studies using  $^{201}\text{Tl}$  (9). In PET imaging, the transfer of patients from treadmill onto the patient bed and then into the tomograph with proper positioning can be difficult, and is, in fact, nearly impossible for short-lived isotopes such as rubidium-82 ( $^{82}\text{Rb}$ ) and  $\text{H}_2^{15}\text{O}$ . A bicycle ergometer peddled by a patient lying in the tomograph is preferable in this case. Many centers using short-lived isotopes will perform rest-dipyridamole studies rather than exercise the patient. In these studies, the resting study is taken first, followed by the injection of dipyridamole and a second study in which dipyridamole induces coronary vasodilation, simulating blood flow during exercise. With short-lived isotopes such as 75-sec half-life  $^{82}\text{Rb}$ , the entire rest-stress or rest-dipyridamole study can be performed within 30–45 min.

## Cardiac Orientation and Re-slicing

The left ventricle can be approximated by an ellipsoid whose long axis lies oblique to the principle-body axes. In single-photon emission computed tomography (SPECT) imaging, it has become customary to analyze cardiac images using image planes that are perpendicular to the left ventricular long axis or “short axis” views (5,10). Each series of short-axis views can be analyzed quantitatively using circumferential-profile analysis and can also be represented schematically in the form of a “bull’s-eye” plot (5).

In PET, unlike SPECT, it has been the convention to design tomographs such that their axial sampling (i.e., slice thickness) is considerably more coarse than their sampling within each slice (i.e., pixel size) (2,11). To obtain short-axis images, these tomographs must either use a combination of gantry tilt and

patient bed angulation to align the patient’s cardiac long-axis to be perpendicular to the scanning planes or mathematically interpolate between the slices (3). Recently, tomographs with finer axial slicing have been developed (12,13), in which case short-axis views can be generated using oblique angle re-slicing software, as in cardiac SPECT. An example of re-sliced cardiac PET images is shown in Figure 1.

## Count Rate Capability

Although many cardiac scans are performed at moderate activity levels, some types of scans require high activity levels, forcing the tomographs to operate at considerably higher count rates than normally experienced. This occurs primarily in two settings:

1. For short-lived isotopes such as  $^{82}\text{Rb}$ , high initial activity levels are required in order to assure that sufficient image counts will be acquired (14). In addition, certain imaging protocols require that the myocardial image be taken in a relatively short period (i.e., a myocardial “snapshot”) in order to assure quantitative accuracy (15,16).
2. Certain quantitative imaging protocols, such as the measurement of myocardial blood flow using  $\text{H}_2^{15}\text{O}$ , require a knowledge of the arterial as well as myocardial tracer concentration. The concentration of tracer in the arterial blood is known as the “arterial input function,” (17,18) which in myocardial imaging can be measured from a dynamic series of images of the ventricular cavity taken immediately following injection. Because all of the injected isotope passes through the ventricle at nearly the same time, even modest bolus injections of tracer result in activity levels in the tomograph which far exceed the levels encountered in other types of PET imaging.

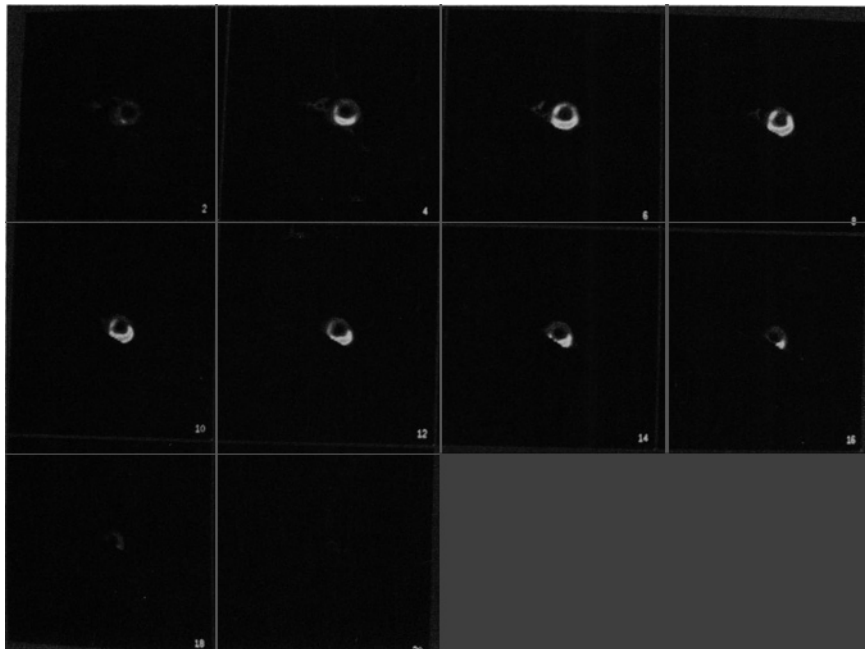


**FIG. 2.** Re-sliced cardiac PET scan images showing the short-axis views.

At high count rates, PET images tend to be degraded by the following three effects:

1. All PET systems take a finite amount of time to detect and record events, during which time additional events will not be able to be detected or recorded. This effect is known as "dead-time," and it results in a loss of data at high count rates (19).
2. In some detection systems, especially those using crystal-to-photomultiplier encoding schemes, detector performance degrades with count rate, (20–22) resulting in image distortions and/or losses in spatial resolution.
3. At high data rates, unrelated photons (i.e., not from the same annihilation) occur closely spaced enough in time to appear to be coincidences. These events are termed "random or accidental coincidences," and they degrade image contrast and increase image noise (23). Random coincidence correction schemes can recover the loss of contrast but cannot eliminate the noise added by random coincidences (23).

Although different tomographs differ in their ability to handle high data rates, in general, image quality is poorer and quantitative accuracy less reliable in high count rate images in comparison to studies taken at more modest count rates. In the selection of imaging protocols, this fact must be weighed against the convenience and unique physiologic properties offered by certain short-lived isotopes such as  $^{82}\text{Rb}$  and  $^{15}\text{O}$ .

### Quantitative Imaging Considerations

In the analysis of cardiac PET images, a number of potential quantitative errors must be considered. This is especially true in the case of those studies aimed at reporting physiologic properties in absolute units; i.e., ml/min/g tissue as in the case of blood flow. The body stops many annihilation photons

on their way to the detectors; therefore, any quantitative imaging protocol must take attenuation into account in order to deduce the tracer concentration in internal organs accurately (4). The assumption of uniform body attenuation, often applied in emission computed tomography, is a poor one in the thorax, where lungs, muscle, ribs and spine result in considerably inhomogeneous attenuation on the body (24). The most accepted technique for attenuation correction is to perform a short transmission scan prior to imaging using an external radioactive source (19). Recently, investigators have demonstrated that it is possible to acquire these scans after the injection of tracer, or even simultaneously with the acquisition of the emission scan saving considerable time in the imaging protocol.

Many of the annihilation photons that interact with the body will scatter by the Compton effect (19). If one of these scattered photons is detected in coincidence with its opposing annihilation photon, the tomograph will record errant information about the location where positron emission occurred. The resulting background counts from these "scattered coincidences" cause quantitative inaccuracies. Scatter must therefore be limited either through the use of inter-plane scatter septa (8) or energy thresholding (7). Many investigators implement scatter correction schemes as well (24).

One additional quantitative consideration is that PET tomographs have a finite ability to spatially resolve the myocardium and the ventricular cavities (25). This is especially true considering that the myocardium and chambers are constantly moving throughout image acquisition. The result is that some of the activity in the myocardium can be placed into the ventricular cavity and vice-versa by the imaging process. This process is termed "spillover" and must be corrected for in those quantitative imaging protocols in which activity is present to any great extent in both the blood pool and the myocardium; for example, in the estimation of the

arterial input concentration from ventricular activity during the period immediately following injection (17,18). Systolic/diastolic gating to tomographically “freeze” the cardiac motion may be helpful in minimizing spillover.

### SPECIFIC TYPES OF PET IMAGING STUDIES

A list of the physiological parameters measured by cardiac PET is given in Table 1, along with the isotopes commonly used in each type of study. Detailed descriptions of each class of study is given below.

#### Myocardial Blood Flow

One of the principal contributions of nuclear medicine to cardiac diagnostics has been the ability to measure regional myocardial blood flow. Unlike other cardiac diagnostic techniques, nuclear tracer methods measure flow at the tissue level, thus the term myocardial “perfusion” studies. Cardiac PET offers an array of cardiac flow tracers which have a number of advantages over single-photon flow agents, including the following (14,16,26–30).

1. Improved image quality and detection of small abnormalities of blood flow.
2. Improved quantitation of blood flow.
3. Reduced sensitivity to artifacts from the attenuation of overlying tissue, such as the diaphragm or the breast.
4. More convenient rest/stress imaging protocols with shorter imaging times.

The various available agents all have one or more of the attractive properties listed above; however, unfortunately, no single agent combines all these features in an optimal way. The choice of flow agent depends upon the availability of an on-site cyclotron and the need for absolute quantification of blood flow. The properties of the different types of flow agents are discussed in this section along with a brief discussion of tracer physiology. Although many PET cardiac flow tracers have been investigated, we will concentrate on the most

frequently used tracers from three classes of compounds: (a) the potassium ( $K^+$ ) analogs, (b) the freely diffusible inert tracers, and (c) a recently developed microsphere-like agent. A list of compounds discussed, along with their pertinent properties, is given in Table 2.

*Potassium Analogs.* An important class of flow agents is the set of cationic tracers which are taken up by the myocardium in analogy to potassium, via different ion transport mechanisms (31–35). The single-photon agent,  $^{201}Tl$ , falls into this category (31,32). These tracers are partially extracted by the myocardium, rapidly cleared from the blood pool after injection and retained by the myocardium for a sufficiently long time to permit imaging. To obtain an absolute measure of blood flow, one needs to know the myocardial tissue concentration, obtained from the myocardial PET image, as well as the arterial concentration, which can be obtained from the infusion-phase ventricular image. Alternatively, relative blood flow can be obtained simply from the myocardial tracer image alone since the arterial input concentration is the equal for all myocardial tissue. Unfortunately, reliable absolute quantitation using the potassium analogs requires a knowledge of the percentage of the tracer taken up by the myocardium or “extraction fraction”, which can vary with flow, falling off at high flow extremes and under conditions of ischemia (31,32,36–40). Although attempts have been made to quantify the extraction fraction as part of the imaging protocol (14), the variability of the extraction fraction makes absolute quantification of myocardial blood flow using potassium analogs difficult. As the multitude of  $^{201}Tl$  users will attest, however, this does not diminish the clinical utility of the potassium analogs. In fact, the reduction of extraction with ischemia helps to highlight defects in myocardial perfusion that may require therapeutic intervention.

The two most commonly used PET Potassium-analogs are  $^{82}Rb^+$  and  $^{13}NH_3$ , where the latter exists in the blood predominantly as  $^{13}NH_4^+$ . Of the two,  $^{82}Rb$  has the advantage in that it is generator-produced, enabling cardiac PET flow imaging without an on-site cyclotron. It would also, therefore, be available on an urgent basis without 24-hr staffing of an on-site isotope production facility. Its short half-life (78 sec) makes back-to-back rest and stress studies feasible; however, because of limited imaging time, the stress state is best accomplished using dipyridamole rather than exercise (27,28,41–49). To its disadvantage, the relatively high count rates experienced in  $^{82}Rb$  imaging, together with its relatively long positron range (distance from emission to annihilation), result in slightly lower image quality in comparison to images obtained using tracers such as  $^{13}NH_3$  and fluorine-18-deoxyglucose ( $^{18}FDG$ ).

An alternative to  $^{82}Rb$  is the tracer,  $^{13}NH_3$ , which is transported into the myocardium largely as  $^{13}NH_4^+$  (29,30,39,40,50–52). Its fate once inside myocardial cells is not completely understood; however, it is postulated that at least some of the tracer is trapped metabolically as amine groups on intracellular compounds (39,40), making its extraction fraction potentially dependent on the metabolic state of the myocardium. Its 10-min half-life makes it possible to take

**TABLE 1. Physiological Parameters Measured by Cardiac PET and Associated Isotopes**

<b>Blood Flow</b>	
Myocardial perfusion	$^{82}Rb^+$ , $^{13}NH_3$ , $^{62}Cu$ -PTSM, $H_2^{15}O$
Blood-Pool imaging	$C_{15}O$ , $^{68}Ga$ -transferrin
<b>Metabolism</b>	
Glucose	$^{18}F$ -fluorodeoxyglucose, $^{11}C$ -deoxyglucose
Fatty acid	$^{11}C$ -palmitate and other $^{11}C$ -fatty acids
Oxidative	$^{11}C$ -acetate
<b>Other</b>	
Pre-synaptic adrenergic innervation	$^{18}F$ -metaraminol, $^{11}C$ -hydroxyephedrine
Tissue viability	$^{18}F$ -misonidazole or $^{18}F$ -fluorodeoxyglucose + flow agent
$\beta$ -receptors	CGP—12177

**TABLE 2. Properties of Selected PET Flow Tracers**

Tracer	Half-life	Production	Uptake Mechanism	Typical Dose
$^{82}\text{Rb}^+$	78 sec	Rb/Sr generator ( $T_{1/2} = 25$ days)	Potassium analog	30–50 mCi
$^{13}\text{NH}_3$	10 min	Cyclotron	Potassium analog	10–20 mCi
$\text{H}_2^{15}\text{O}$	2 min	Cyclotron	Freely diffusible tracer	30–50 mCi
$^{62}\text{Cu-PTSM}$	10 min	Cu/Zn generator	“Chemical microsphere”	10 mCi
$\text{C}^{15}\text{O}$	2 min	Cyclotron ( $T_{1/2} = 9$ hr)	Blood-pool agent	30–50 mCi

images at lower count rates than with  $^{82}\text{Rb}$ ; however, since it is a cyclotron-produced compound,  $^{13}\text{NH}_3$ , must be produced on-site, as its half-life precludes delivery from a regional isotope production facility.

*Freely diffusible inert tracers.* A second class of flow tracers enters and exits the myocardium freely by passive diffusion; thus, tracer concentration equilibrates rapidly between blood and tissue. The measurement of blood flow using this class of tracers is based upon the model originally used to measure regional cerebral blood flow (15). Tracer is taken up by the myocardium depending upon flow and the relative affinity of the tracer for myocardial tissue versus blood,  $\lambda$ , the partition coefficient. Unlike the extraction fraction, known as the partition coefficient is a function only of the chemical properties of the blood and tissue and is not dependent upon flow or metabolic status.

In practical imaging using freely diffusible tracers, it is desirable to measure blood flow using a nearly instantaneous or bolus injection of isotope followed by a short imaging period at the time the tracer reaches the myocardium. This bolus technique has been shown to be advantageous with respect to its accurate quantitation of blood flow; however, it results in the need to count at high rates (15,16,53). Furthermore, one must obtain tomographic images at a time when the tracer is present both in the ventricle and the myocardium, with resulting spillover in image counts. One technique for handling the problem is to obtain a corresponding blood-pool image using an agent such as  $\text{C}^{15}\text{O}$  (16,54,55). If both the blood-pool and perfusion scans are performed with similar activity levels, then the blood-pool image can be subtracted from the perfusion image to yield an image of the myocardium (see Figure 3). Alternate techniques which use the time-varying nature of the freely diffusible tracer distribution to separate blood-pool activity from myocardial activity are being investigated (55–57).

The agent of choice among freely diffusible tracers is  $\text{H}_2^{15}\text{O}$ . Water is an inert, stable substance that easily moves throughout all tissues. The short-half life of  $^{15}\text{O}$  (~2 min) requires not only an on-site cyclotron but also special isotope delivery systems to assure prompt transport of the isotope from the cyclotron to the imaging facility. The tracer is usually administered as an i.v. bolus; frequently preceded by an inhalation of  $\text{C}^{15}\text{O}$  to delineate the blood pool (15,55). Like  $^{82}\text{Rb}$ , the short half-life of  $\text{H}_2^{15}\text{O}$  allows back-to-back studies; however, unlike  $^{82}\text{Rb}$ , the constancy of the tissue-blood partition coefficient for water eliminates the variability of extraction and avoids systematic errors in the calculation of absolute blood

flow (16,55). Unfortunately, short imaging times with high count rates and the need to subtract two separate studies result in myocardial images that are usually inferior in quality to those obtained using the potassium-analog tracers. The recent development of low-cost oxygen-only accelerators has spurred interest in the use of  $\text{H}_2^{15}\text{O}$  as a clinical flow tracer, and techniques for measuring myocardial blood flow other than bolus injection have been investigated (57). Currently, however, most clinical studies are performed using  $^{82}\text{Rb}$  or  $^{13}\text{NH}_3$ , with  $\text{H}_2^{15}\text{O}$  reserved for those institutions undertaking research in which more rigorously quantitative measures of regional myocardial blood flow are necessary.

*c. Microsphere-like agents.* The “gold standard” in experimental measurements of organ blood flow has been the use of radiolabeled microspheres (58). The ideal microspheres have the following properties:

1. They are 100% extracted from the blood-pool on the first pass through the capillary bed.
2. They are retained in the capillary bed without washout for a period of time sufficient to permit the measurement of their distribution.

Given this set of properties, the blood flow is readily calculated from the tissue concentration and the arterial input concentration of microspheres.

Unfortunately, although PET-labeled microspheres have been shown to represent myocardial blood flow accurately, (58) the action of blocking a fraction of the capillaries in the myocardium, especially in patients who frequently already have compromised myocardial blood flow, makes positron-emitting microspheres somewhat untenable. Recently, Green et al. (59) have shown that the copper-labeled compound copper(II)pyruvaldehyde bis( $\text{N}^4$ -methylthiosemicarbazone) (Cu-PTSM) behaves like a “chemical microsphere” in that it is retained in a stable manner for a long period of time. Labeled with the positron emitter  $^{62}\text{Cu}$ , available from a Cu/Zn generator (parent half-life = 9 hr),  $^{62}\text{Cu-PTSM}$  could be made available on a regional basis, even to those institutions without cyclotrons (60,61). While early experiments with this compound are promising (62), more work is needed to fully characterize its properties as a myocardial flow tracer.

### Myocardial Metabolism

The distinction between viable but functionally impaired myocardium is important in the management of patients with

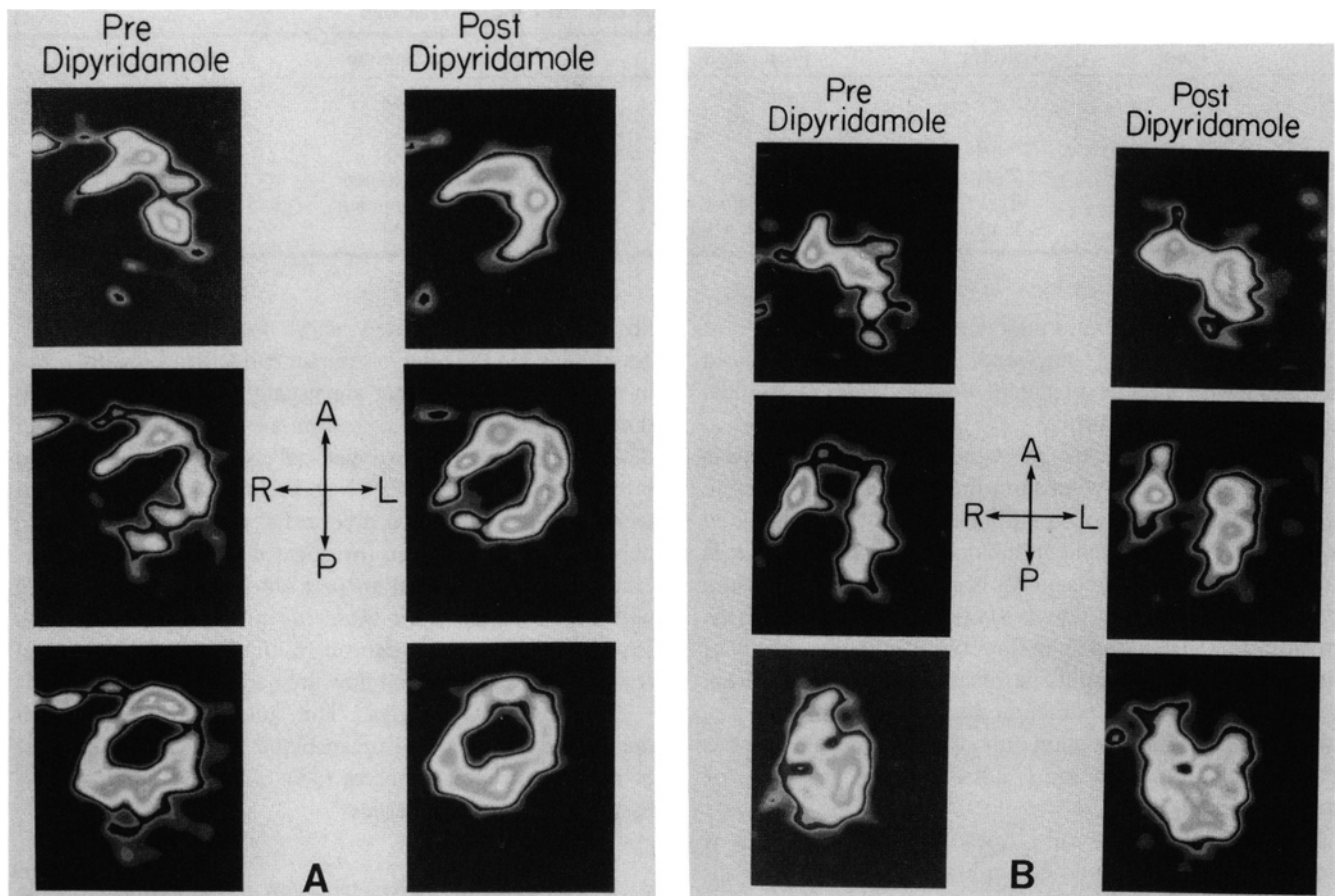


**FIG. 3.** Tomograms of  $H_2O^{15}$  flow study from a normal subject (A) and from a patient with a significant occlusion of the LAD coronary artery (B). Both images are before (left) and after (right) administration of dipyridamole. (Photographs provided courtesy of Drs. M. N. Walsh and S. R. Bergmann, Cardiovascular Division, Washington University, St. Louis.)

ischemic heart disease in whom coronary revascularization procedures are being considered. Myocardial metabolic activity is an essential feature of myocardial viability. The presence of active metabolism in regions of myocardium supplied by occluded or stenosed coronary arteries provides evidence of jeopardized ischemic myocardium. At present, only indirect information regarding myocardial viability can be obtained by using coronary artery flow tracers such as  $^{201}Tl$  or assessments of regional left ventricular wall motion. Metabolic imaging using PET provides a unique approach for the identification of viable myocardium. Prior studies in both animals and human subjects have demonstrated the utility of PET with  $^{18}F$ -2-deoxyglucose and  $^{11}C$ -acetate for assessing myocardial metabolic activity in vivo.

*Limitations of Thallium-201 Myocardial Scintigraphy.* At present,  $^{201}Tl$  scintigraphy is the most frequently used imaging technique for the clinical assessment of myocardial viability (63,64). However,  $^{201}Tl$  perfusion scans provide only an indirect assessment of myocardial viability. Patients are evaluated with thallium imaging obtained immediately after exercise and three hours later, while at rest. Perfusion defects seen with exercise which disappear 3–4 hr later are felt to be indicative of ischemia and suggest the presence of viable myocardium. Fixed perfusion defects seen both after exercise and three hours later are generally classified as infarctions or

scars (65,66). This term implies the absence of viable myocardium. However, such images are frequently observed in the absence of a prior history or clinical or electrocardiographic evidence of myocardial infarction. In fact, repeat thallium imaging obtained 18–72 hr after exercise, or after re-injection, may show partial redistribution of thallium in these defects, indicating the presence of viable myocardium. In a study by Kiat et al., 64% of segments with persistent SPECT thallium defects at four hours exhibited redistribution 18–72 hr later (68). They reported that 95% of segments with late reversibility showed an improved thallium perfusion pattern after coronary revascularization, while only 37% of the segments with late, nonreversible defects demonstrated an improvement (67). The presence of late thallium redistribution indicates that although there is severely diminished coronary blood flow, viable myocardium is present. Thallium-201 imaging thus overestimates the extent of scar tissue. Recent quantitative planar thallium scintigraphic studies by Gibson et al. have shown that up to 43% of myocardial segments with persistent thallium defects exhibited normal perfusion pattern and normal thallium kinetics after coronary revascularization (68). Thus, these observations highlight the limitations of the 4-hr nonreversible  $^{201}Tl$  defect as a marker of nonviable myocardium. Cardiac PET provides a more direct assessment of myocardial metabolism as well as a method of

determining the presence of viable myocardium in regions with fixed or partially reversible perfusion defects (69).

**Myocardial Metabolic Imaging.** Myocardial metabolic imaging can be performed using one of several tracers. The three most commonly used tracers are: (1)  $^{18}\text{F}$ -2-deoxyglucose (FDG) (half-life 109.7 min), which reflects exogenous glucose metabolism; (2)  $^{11}\text{C}$ -acetate (half-life 20.4 min), which measures myocardial oxidative metabolism; and (3)  $^{11}\text{C}$ -palmitate (half-life 20.4 min.) which traces mitochondrial fatty acid oxidation.

**Flourine-18-2-Deoxyglucose.** Fluorodeoxyglucose (FDG) is a biochemical marker for the initial step of glycolysis. It is transported from the blood into the myocardium in proportion to plasma glucose and then competes with glucose for the enzyme hexokinase. The phosphorylated tracer, FDG-6-phosphate, becomes trapped in myocardial cells for three reasons:

1. Cell membranes are impermeable to FDG.
2. Unlike glucose-6-phosphate; FDG is a poor substrate for glycogen synthesis, glycolysis and the pentose phosphate shunt.
3. Dephosphorylation of FDG is slow.

In aerobic myocardium, free fatty acids are the predominant fuel source; in ischemic myocardium, glucose becomes a more important substrate due to a shift toward anaerobic glycolysis (70). Marshall et al. have demonstrated that the ratio of FDG trapped in myocardium relative to unlabeled glucose does not vary in either low flow or demand-induced ischemia (71). Delineation of myocardial perfusion and metabolism allows the differentiation of viable myocardium from scar tissue. Myocardial perfusion assessed by  $^{201}\text{Tl}$  with SPECT, or  $^{13}\text{N}$ -ammonia or  $^{82}\text{Rb}$  with PET is decreased in both scar tissue and viable, "hibernating" myocardium. Glucose metabolism is present in viable myocardium yet is absent in scar tissue. The concordance of both decreased blood flow and absent FDG uptake in infarcted, nonviable segments generates a pattern called "blood flow-metabolism match" whereas the dissociation between perfusion and FDG uptake seen in viable but compromised myocardium is referred to as "blood-flow-metabolism mismatch" (70,72) (Figs. 4A and 4B). Brunken et al. have shown persistence of metabolic activity in the majority of myocardial segments with fixed or partially reversible stress thallium defects using PET with  $^{18}\text{F}$ -2-deoxyglucose, implying that flow tracers alone underestimate the extent of viable tissue in hypoperfused myocardial segments (7,11). Of 51 myocardial segments with planar stress thallium defects in 12 patients, myocardial glucose utilization was identified in 21 of 36 (58%) segments with fixed defects and 7 out of 11 (64%) segments with partially reversible defects. The magnitude of the thallium defect and the apparent improvement of the defect four hours after exercise did not differentiate ischemic from infarcted segments. In a separate study of 142 segments analyzed using SPECT, 101 had fixed defects, 31 had partially reversible defects and 10 had completely reversible defects. FDG uptake was observed in

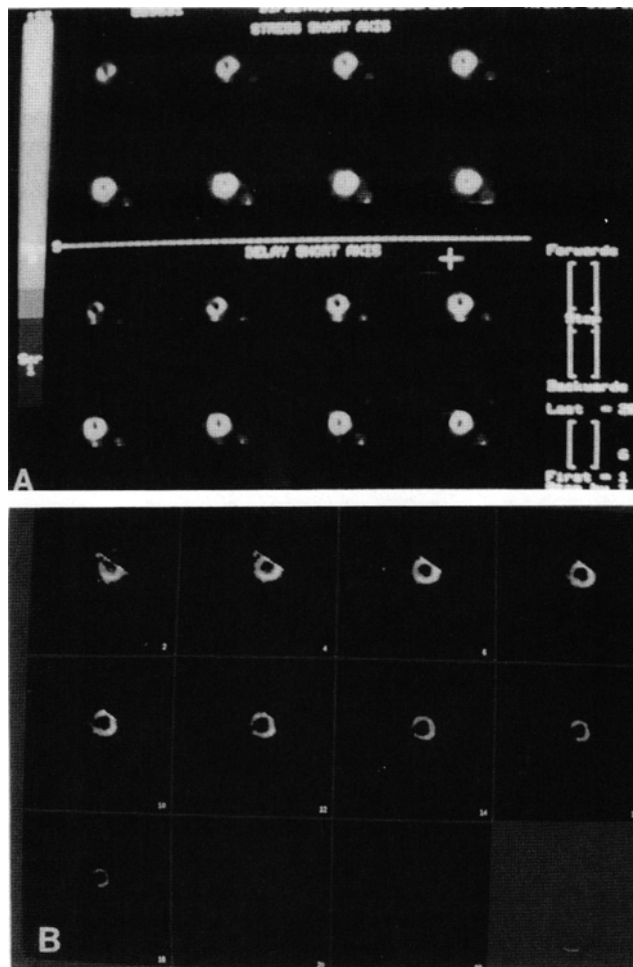


**FIG. 4.** Demonstration of myocardial viability using metabolic PET imaging. Short-axis views of  $^{201}\text{Tl}$  perfusion image (A) and  $^{18}\text{F}$ FDG glucose metabolic image (B) in a patient with a previous myocardial infarction. FDG image shows glucose metabolism where perfusion is absent on both the stress and 4-hr delayed images. This pattern is known as a perfusion-metabolism mismatch and indicates compromised, but viable, myocardium.

47 (46.5%) of the 101 segments with fixed defects, in 20 (64.5%) of the 31 segments with partially reversible defects and in 5 (50%) of the 10 segments with completely reversible defects. The other five segments with completely reversible defects exhibited ischemia on PET. Their data suggest that reliance on SPECT thallium scintigraphic data alone would result in underestimation of the extent of viable tissue in nearly half of myocardial segments with fixed defects and overestimation of the extent of jeopardized tissue in one-third of myocardial segments with partially reversible thallium defects.

Schelbert and co-workers have demonstrated the unreliability of commonly used clinical tests in distinguishing viable from infarcted myocardium (74). These investigators have electrocardiographically demonstrated the presence of persistent tissue metabolism, assessed by metabolic imaging with FDG, in a high proportion (54%) of myocardial regions with evidence of chronic Q-wave infarction. Their findings indicate that infarcted regions, defined by conventional methods, still

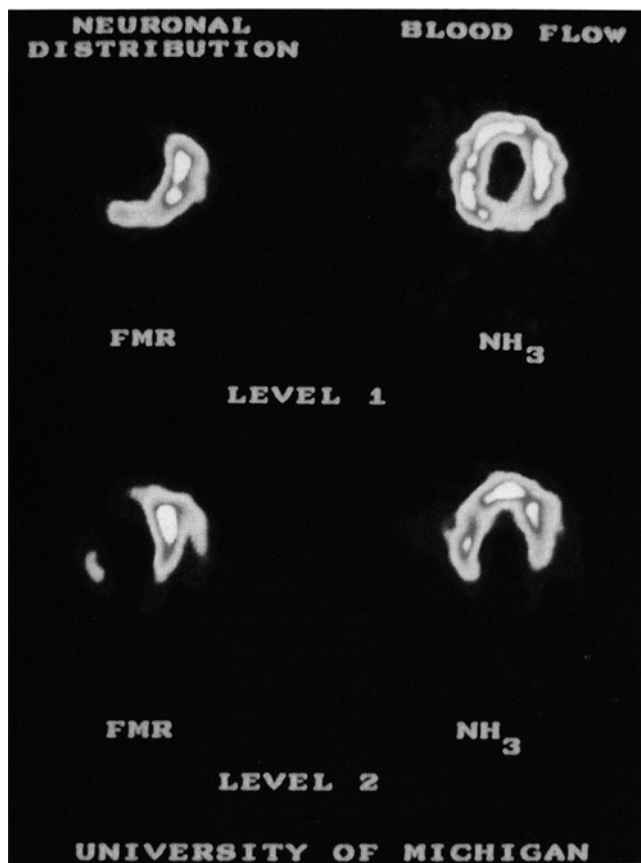


**FIG. 5.** Imaging the adrenergic innervation of the heart using  $^{18}\text{F}$ -metaraminol. Transverse myocardial images of perfusion using  $^{13}\text{N}$ - $\text{NH}_3$  (right) and adrenergic innervation using  $^{18}\text{F}$ -metaraminol (left) on a dog whose cardiac innervation has been damaged by the application of phenol. The unmatched defect in the metaraminol image demonstrates that the adrenergic nervous system is no longer functioning in a region where innervation was interrupted but where perfusion was not. (Photo courtesy of Drs. Wieland and Hutchins, Division of Nuclear Medicine, University of Michigan.)

have viable tissue that may recover function following revascularization. Schwaiger et al. have shown that PET demonstrates a high incidence of residual tissue viability in ventricular segments with diminished flow and impaired function during the subacute phase of myocardial infarction (75). PET is more suitable for determining size of an infarct and differentiates functionally impaired but viable from irreversibly injured necrotic myocardium.

Tillisch et al. have shown that cardiac PET imaging, with  $^{13}\text{N}$ - $\text{NH}_3$  to assess coronary blood flow and  $^{18}\text{F}$ -FDG to assess metabolic viability, is an accurate method of predicting potential reversibility of wall-motion abnormalities after surgical revascularization (72). They used PET to predict improvement in left ventricular wall motion abnormalities preoperatively in 17 patients who underwent coronary-artery bypass surgery. FDG imaging with PET demonstrated a 92% predictive value for improvement in myocardial wall motion following surgical revascularization (76). Other investigators have also shown that preoperative metabolic FDG imaging using PET is useful for predicting the response to coronary artery

bypass graft surgery (CABG) (77). Thus, hypoperfused, dysfunctional myocardial segments (referred by some investigators as "stunned myocardium"), with increased uptake of FDG, are still viable and may recover contractile function when coronary blood flow is restored.

Metabolic imaging is also useful to assess the extent of viable myocardial tissue in patients with severe left ventricular dysfunction. This determination is particularly important before coronary revascularization. Mody et al. have shown that metabolic imaging can distinguish idiopathic from ischemic cardiomyopathy. They demonstrated relatively homogenous blood flow and glucose utilization in idiopathic cardiomyopathy whereas in ischemic cardiomyopathy, 50% of hypoperfused regions were infarcted by PET criteria and the remaining 50% had preserved glucose metabolism (78).

*Limitations of FDG.* FDG imaging has two major limitations: (1) uptake upon the dietary state and; (2) it only reflects the initial step of glucose metabolism. The major substrates for myocardial metabolism are free fatty acids. Fluorine-18-2-deoxyglucose as a metabolic tracer has limitations since glucose is a secondary source of energy generation in myocardium. After an oral glucose load, i.v. FDG is trapped by viable but not necrotic myocardial cells. However, after 12 hr of fasting, FDG is trapped by ischemic but not by normal myocardium or scar. Thus, to accentuate myocardial glucose uptake and metabolism relative to that of free fatty acids, 50 g of an oral glucose load is usually given prior to imaging. This results in increased FDG uptake throughout the myocardium, including ischemic zones, and thereby facilitates PET imaging. FDG has another limitation as a metabolic tracer in that it does not reflect glucose metabolism beyond phosphorylation by hexokinase. Glucose flux from glycogen synthesis or glycolysis is not measured by FDG imaging.

*Carbon-11-Acetate Metabolic Imaging.* Myocardial metabolism can also be measured using PET with  $^{11}\text{C}$  as an imaging agent. Recent studies employed  $^{11}\text{C}$ -labeled acetate to trace tricyclic acid cycle (TCA) flux and therefore oxidative metabolism directly (79-85). Acetate labeled with  $^{11}\text{C}$  is activated by  $^{11}\text{C}$ -acetyl CoA, which is predominantly metabolized to  $^{11}\text{CO}_2$  through the TCA cycle. Since the TCA cycle is tightly coupled to oxidative phosphorylation, the kinetics of  $^{11}\text{C}$ -acetate oxidation in myocardial tissue provide an index of oxidative metabolism. Brown and co-workers have shown that externally detectable clearance of  $^{11}\text{C}$ -labeled acetate provides an accurate quantitative index of myocardial oxidative metabolism ( $\text{MVO}_2$ ) in a canine preparation (79,81). This finding is supported by three observations:

1. The rate of clearance of  $^{11}\text{C}$  radioactivity, obtained from the decay characteristics of myocardial time-activity curves, is closely correlated with  $\text{MVO}_2$  ( $r = 0.90$ ) as well as with the rate-pressure product ( $r = 0.95$ ).
2. 98% of the  $^{11}\text{C}$ -activity detected in the coronary sinus was in the form of  $^{11}\text{CO}_2$ , a by-product of TCA cycle activity.
3. No significant difference was found between the rate of clearance of  $^{11}\text{C}$  radioactivity by PET and the myocardial

efflux of  $^{11}\text{C}\text{O}_2$  measured directly from the coronary sinus.

Their study showed that the estimation of  $\text{MVO}_2$ , derived from the rate of oxidation of  $^{11}\text{C}$ -acetate, can be assessed noninvasively by PET under diverse physiological conditions and over a wide range of flow and metabolic states despite changes in myocardial substrate utilization. This would potentially be useful in delineating the distribution and amount of jeopardized myocardium. Human studies, using  $^{11}\text{C}$ -acetate as a noninvasive marker of regional  $\text{MVO}_2$  with dynamic PET, have shown high quality images in both normal volunteers (84) and in patients with transmural myocardial infarction (85). The effects of acute interventions on regional myocardial oxidative metabolism are unknown. The extent of recovery of myocardial oxidative metabolism after coronary thrombolysis can be accurately quantitated using PET with  $^{11}\text{C}$ -acetate as a metabolic tracer (86). This imaging modality may thus allow the noninvasive evaluation of the efficacy of such interventions.

To more accurately reflect myocardial metabolism, particularly oxidative metabolism, another metabolic tracer is therefore required. Carbon-11-acetate myocardial turnover has been shown by investigators to provide excellent estimations of regional myocardial metabolism. As this tracer is directly incorporated into the TCA cycle and is metabolized to an end-product of metabolism ( $\text{CO}_2$ ), the limitations of using FDG to assess metabolism are circumvented. Carbon-11-acetate uptake and metabolism are not affected by substrate administration and the high extraction fraction of  $^{11}\text{C}$ -acetate is essentially independent of flow and ischemia. Therefore,  $^{11}\text{C}$ -acetate can be used in conjunction with FDG to assess both oxidative metabolism and glycolysis. Finally, severely ischemic myocardium may exhibit decreased glycolysis, yet may be viable. As a result, FDG uptake may be decreased in ischemic myocardium and PET will underestimate viable myocardium using this tracer alone. Carbon-11-acetate imaging provides a method of circumventing this problem.

**Carbon-11-Palmitate.** Carbon-11-palmitate is a tagged 16-carbon long-chain fatty acid that reflects mitochondrial fatty acids oxidation. Its use as a metabolic tracer is limited because both its uptake and clearance are affected by several factors. Rosamond et al. have demonstrated in an open-chest dog model that back-diffusion of non-metabolized  $^{11}\text{C}$ -palmitate from myocardium into the vascular space occurs in ischemic tissue (87). Therefore, during ischemia externally detected clearance rates cannot be used to quantitate fatty acid metabolism, at least with the currently used parameter estimation techniques.

### Other Types of Studies

**Myocardial Adrenergic Innervation.** The role of perturbations in myocardial adrenergic innervation is unknown. Experimental studies in animals have demonstrated that denervated myocardium may be electrically unstable (88,89). It is known from studies in animals and patients that abnormal myocardial innervation can occur as a result of myocardial

infarction (90,91) and cardiomyopathy (92,93). Imaging studies have used iodine-123-labeled metaiodobenzylguanidine to assess myocardial adrenergic innervation. More recently, analogs of catecholamines labeled with positron emitting radioisotopes have been used to assess myocardial adrenergic innervation. These agents share the uptake, storage and release mechanisms of norepinephrine in the presynaptic nerve terminals. Fluorine-18-fluorometaraminol (FMR) has been shown by Hutchins and colleagues to provide evidence of myocardial denervation in experimental animals with myocardial infarction (Fig. 5) (94). The extent of denervation and the myocardial content of FMR correlated well with the degree of norepinephrine depletion. Clinical studies by Schwaiger using another analog,  $^{11}\text{C}$ -hydroxyephedrine, showed that uptake of this agent is homogeneous in normal volunteers but is absent in patients with cardiac transplants (these patients have absent myocardial innervation) (95). More extensive studies using this technique will no doubt be forthcoming.

**Receptor Imaging.** Adrenergic receptors play a significant role in mediating the effects of catecholamines on myocardial cells. They are responsible for the increased contractility and heart rate resulting from catecholamines. The quantity of cardiac adrenergic receptors is altered in diseases such as cardiomyopathy.

Imaging of myocardial adrenergic receptors has been difficult in the past as these receptors are present not only in the heart but in the lungs. Recently, investigators have developed a ligand, CGP-12177, which has strong affinity for myocardial adrenergic receptors and can be labeled with positron-emitting isotopes (96). The heart is also innervated by the parasympathomimetic nervous system. This network of nerves is responsible for maintaining coronary artery tone and for slowing the heart rate. Receptors for these nerves bind acetylcholine. Two tracers have been developed which bind to these receptors.  $^{11}\text{C}$ -methyl-QNB has been shown to have extensive cardiac uptake (97). Tropyllbenzilate methiodide (MTRB), the second tracer, is presently undergoing experimental investigation in animals (98). Though highly promising, much work remains to be done with these agents.

**Misonidazole.** Bergmann and colleagues at Washington University have studied  $^{18}\text{F}$ -misonidazole, an agent avidly taken up by hypoxic but non-necrotic myocardium. This agent has been used both in isolated hearts and, more recently, in dogs (99,100). This work has demonstrated that ischemic myocardium has greater extraction of this tracer agent than normal myocardium. Imaging with  $^{18}\text{F}$ -misonidazole and PET may therefore offer the ability to detect viable but jeopardized myocardium and allow for early therapeutic interventions.

### CONCLUSION

PET is a highly versatile imaging technique which can provide noninvasive assessment of in vivo myocardial metabolism, myocardial tissue perfusion and, ultimately myocardial innervation and receptors. Future developments may include labeling of monoclonal antibodies with positron-emitting iso-

topes to image a variety of cardiovascular phenomena. Although most of the present work is investigational, metabolic and flow imaging have been used in clinical investigations. Imaging with PET can provide relatively unique information, such as assessment of myocardial metabolism and hence, viability and may provide more definitive information, including quantitative data on coronary artery blood flow than is available with SPECT. The importance of PET for cardiovascular research has already been well established and new applications for this technique will continue to be developed. Direct application to patient care such as assessment of myocardial viability and efficacy of therapeutic intervention may establish PET as a clinically important diagnostic tool.

## REFERENCES

- Muehllehner G, Karp JS. Positron Emission Tomography—technical considerations. *Semin Nucl Med* 1986;16:35–50.
- Brooks RA, Sank VJ, Friauf WS, et al. Design considerations of positron emission tomography. *IEE Trans Biomed Eng* 1981;BME-28:158–177.
- Budinger TF, Yano Y, Huesman RH, et al. Positron emission tomography of the heart. *Physiologist* 1983;26:31–34.
- Budinger TF, Gullberg GT, Huesman RH. Emission computed tomography. In: Herman GE, ed. *Topics in applied physics. Image reconstruction from projections*. New York: Springer-Verlag; 1979.
- Garcia EV, Train KV, Maddahi J., et al. Quantification of rotational thallium-201 myocardial tomography. *J Nucl Med* 1985;26:17–26.
- Derenzo SE, Zaklad H, Budinger TF. Analytical study of a high-resolution positron ring detector system for transaxial reconstruction tomography. *J Nucl Med* 1975;16:1166–1173.
- Mankoff D, Muehllehner G. Performance of positron imaging systems as a function of energy threshold and shielding depth. *IEEE Trans MED Imag* 1984;M1-3:18–24.
- Derenzo SE. Method for optimizing side shielding in positron emission tomographs and for comparing detector materials. *J Nucl Med* 1980;21:971–977.
- Gerson MC, Thomas SR, Van Heertum R. Tomographic myocardial perfusion imaging. In: Gerson MC, ed. *Cardiac nuclear medicine*. New York: McGraw-Hill; 1987: 25–52.
- Borrello JA, Clinthorne NH, Rogers WL, et al. Oblique angle tomography: A reconstruction algorithm for transaxial tomographic data. *J Nucl Med* 1981;22:471–473.
- Karp JS, Daube-Witherspoon MD, Muehllehner G. Factors affecting accuracy and provision in PET volume imaging. *J Cereb Metab Blood Flow*. 1990; in press.
- Hicks K, Ganti G, Mullani N, Gould KL. Automated quantitation of three-dimensional cardiac positron emission tomography for routine clinical use. *J Nucl Med* 1989;30:1787–1797.
- Karp JS, Muehllehner G, Mankoff D, et al. Multi-slice PennPET: a positron tomograph with volume-imaging capability. *J Nucl Med* 1990;31:617–627.
- Mullani NA, Goldstein RA, Gould KL, et al. Myocardial perfusion with rubidium-82 I. Measurement of extraction fraction and flow with external detectors. *J Nucl Med* 1983;24:898–906.
- Ter-Pogossian MM, Herscovitch P. Radioactive oxygen-15 in the study of cerebral blood flow, blood volume, and oxygen metabolism. *Semin Nucl Med* 1985;4:377–394.
- Bergmann SR, Fox KA, Rand AL, et al. Quantification of regional myocardial blood flow in vivo with  $H_2^{15}O$ . *Circulation* 1984;4:724–733.
- Weinberg IN, Huang SC, Araujo L, et al. Validation of PET-acquired input functions for cardiac studies. *J Nucl Med* 29:241–247, 1988.
- Henze E, Huang SC, Ratib O, et al. Measurements of regional tissue and blood-pool radiotracer concentration from serial tomographic images of the heart. *J Nucl Med* 1983;24:987–996.
- Knoll GF. *Radiation: detection and measurement*. New York: John Wiley & Sons; 1979.
- Mankoff DA, Muehllehner G, Karp JS. The high count rate performance of a two-dimensionally positron-sensitive detector for positron emission tomography. *Phys Med Biol* 1989;34:437–456.
- Mankoff DA, Muehllehner G, Karp JS. The effect of detector performance on high count rate PET imaging with a tomograph based on positron-sensitive detectors. *IEEE Trans Nucl Sci* 1988;NS-35:592–7.
- Germano G, Hoffman EJ. The effect of pileup in 2-D modular detector systems for multiplane PET imaging [Abstract]. *J Nucl Med* 1989;30:745.
- Hoffman EJ, Huang SC, Phelps ME, et al. Quantitation in positron emission tomography: 4 Effect of accidental coincidences. *J Comput Assist Tomogr* 1981;5:391–400.
- Bergstrom M, Bohm C, Ericson K, et al. Corrections for attenuation, scattered radiation, and random coincidences in a ring detector positron emission transaxial tomograph. *IEEE Trans Nucl Sci* 1980;NS-27:549–554.
- Hoffman EJ, Huang SC, Phelps ME. Quantitation of positron emission computed tomography: effect of object size. *J Comput Assist Tomogr* 1979;3:299–308.
- Mullani NA. Myocardial perfusion with rubidium-82: III. Theory relating severity of coronary stenosis to perfusion defect. *J Nucl Med* 1984;25:1190–1196.
- Go RT, Marwick TH, MacIntyre WJ, et al. Initial results of comparative rubidium-82 and thallium-201 myocardial perfusion imaging in diagnosis of CAD [Abstract]. *J Nucl Med* 1989;30:759.
- Kalus ME, Stewart RE, Gacoch GM, et al. Comparison of Rb-82 PET and Tl-201 SPECT for detection of regional coronary artery disease [Abstract]. *J Nucl Med* 1989;30:829–830.
- Schelbert HR, Phelps ME, Huang SC, et al. N-13 ammonia as an indicator of myocardial blood flow. *Circulation* 1981;63:1259–1272.
- Tamaki N, Yonekura Y, Senda M, et al. Value and limitation of stress thallium-201 single photon emission computed tomography: comparison with nitrogen-13 ammonia positron tomography. *J Nucl Med* 1988;29:1181–1188.
- Leppo JA: Myocardial uptake of thallium and rubidium during alterations in perfusion and oxygenation in isolated rabbit hearts. *J Nucl Med* 1987;28:878–885.
- Welch HF, Strauss HW, Pitt B. The extraction of thallium-201 by the myocardium. *Circulation* 1977;56:188–191.
- Bassingthwaighte JB. A concurrent flow model for extraction during trans-capillary passage. *Circ Res* 1974;35:483–503.
- Tancredi RG, Yipintso T, Bassingthwaighte JB. Capillary and cell wall permeability to potassium in isolated dog hearts. *Am J Physiol* 1975;229:537–544.
- Guller B, Ypintso T, Orvis AI, et al. Myocardial sodium extraction at varied coronary flows in the dog. *Circ Res* 1975;37:359–378.
- Selwyn AP, Allan RM, L'Abbate A, et al. Relation between regional myocardial uptake of rubidium-82 and perfusion: absolute reduction of cation uptake in ischemia. *Am J Cardiol* 1982;50:112–121.
- Becker L, Ferreira R, Thomas M. Comparison of  $^{86}Rb$  and microsphere estimates of left ventricular bloodflow distribution. *J Nucl Med* 1974;15:969–973.
- Knoebel SB, Lowe DK, Lovelace DE, et al. Myocardial blood flow as measured by fractional uptake of rubidium-84 and microspheres. *J Nucl Med* 1978;19:1020–1026.
- Bergmann SR, Hack S, Tewson T, et al. The dependence of accumulation of  $^{13}NH_3$  by myocardium on metabolic factors and its implications for quantitative assessment of perfusion. *Circulation* 1981;61:34–43.
- Rauch B, Frantizek H, Grunze M, et al. Kinetics of  $^{13}N$ -

ammonia uptake in myocardial single cells indicating potential limitations in its applicability as a marker of myocardial blood flow. *Circulation* 1985;71:387-393.

41. Goldstein RA, Mullani NA, Marani SK, et al. Myocardial perfusion with rubidium-82. II. Effects of metabolic and pharmacologic interventions. *J Nucl Med* 1983;24:907-915.

42. Shea MJ, Wilson RA, deLandsheare CM, et al. Use of short- and long-life rubidium tracers for the study of transient ischemia. *J Nucl Med* 1987;28:989-997.

43. Goldstein RA: Kinetics of rubidium-82 after coronary occlusion and reperfusion. Assessment of patency and viability in open-chested dogs. *J Clin Invest* 1985;75:1131-1137.

44. Goldstein RA, Kirkeeide RL, Smalling RW, et al. Changes in myocardial perfusion reserve after PTCA: noninvasive assessment with positron tomography. *J Nucl Med* 1987;28:1262-1267.

45. Goldstein RA, Mullani NA, Wong WH, et al. Positron imaging of myocardial infarction with rubidium-82. *J Nucl Med* 1986;27:1824-1829.

46. Gould KL, Goldstein RA, Mullani NA, et al. Noninvasive assessment of coronary stenoses by myocardial perfusion imaging during pharmacologic coronary vasodilation. VIII. Clinical feasibility of positron cardiac imaging without a cyclotron using generator-produced rubidium-82. *J Am Coll Cardiol* 1986;7:775-789.

47. Kirkeeide RL, Gould KL, Parsel L. Assessment of coronary stenoses by myocardial perfusion imaging during pharmacologic coronary vasodilation. VII. Validation of coronary flow reserve as a single integrated functional measure of stenosis severity reflecting all its geometric dimensions. *J Am Coll Cardiol* 1986;7:103-113.

48. Demer LL, Gould KL, Goldstein RA, et al. Assessment of coronary artery disease severity by positron emission tomography: comparison with quantitative arteriography in 193 patients. *Circulation* 1989;79:825-835.

49. Brown BG, Josephson MA, Petersen RB, et al. Intravenous dipyridamole combined with isometric handgrip for near maximal acute increase in coronary flow in patients with coronary artery disease. *Am J Cardiol* 1981;48:1077-1085.

50. Tamaki N, Senda M, Yonekura Y, et al. Dynamic positron computed tomography of the heart with a high sensitivity positron camera and nitrogen-13 ammonia. *J Nucl Med* 1985;26:567-575.

51. Shah A, Schelbert HR, Schwaiger M, et al. Measurement of regional myocardial blood flow with N-13 ammonia and positron-emission tomography in intact dogs. *J Am Coll Cardiol* 1985;5:92-100.

52. Tamaki N, Yonekura Y, Yamashita K, et al. Value of rest-stress myocardial positron tomography using nitrogen-13 ammonia for the preoperative prediction of reversible asynergy. *J Nucl Med* 1989;30:1302-1310.

53. Huang SC, Schwaiger M, Carson RE, et al. Quantitative measurement of myocardial blood flow with oxygen-15 water and positron computed tomography: an assessment of potential and problems. *J Nucl Med* 1985;26:616-625.

54. Walsh MN, Bergmann SR, Steele RL, et al. Delineation of impaired regional myocardial perfusion by positron emission tomography with H<sub>2</sub><sup>15</sup>O. *Circulation* 1988;78:612-620.

55. Bergmann SR, Hererro P, Markham J, et al. Noninvasive quantitation of myocardial blood flow in human subjects with oxygen-15-labeled water and positron emission tomography. *J Am Coll Cardiol* 1988;14:639-652.

56. Bacharach SL, Cuocola A, Bonow RO, et al. PET myocardial blood flow by H<sub>2</sub><sup>15</sup>O without a blood pool scan. *J Nucl Med* 1989;30:807.

57. Lammertsma AA, Araujo LI, McFalls EO. A new method to quantitate regional myocardial blood flow. *J Nucl Med* 1989;30:808.

58. Wilson RA, Shea MJ, deLandsheare CM, et al. Validation of quantitation of regional myocardial blood flow in vivo with 11-C-labeled human albumin microspheres and positron emission tomography. *Circulation* 1984;4:747-723.

59. Green MA, Klippenstein DL, Tennison JR. Copper (II) bis

(thiosemicarbazone) complexes as potential tracers for evaluation of cerebral and myocardial blood flow with PET. *J Nucl Med* 1988;29:1549-1557.

60. Yagi M, Kondo K. A <sup>62</sup>Cu generator. *Int J App Radiat Isot* 1979;30:569-570.

61. Robinson GD Jr, Zielinski FW, Lee AW. The zinc-62/copper-62 generator: a convenient source of copper-62 for radiopharmaceuticals. *Int J App Radiat Isot* 1980;31:111-116.

62. Shelton ME, Green MA, Mathias CJ, et al. Kinetics of copper-PTSM in isolated hearts: a novel tracer for measuring blood flow with positron emission tomography. *J Nucl Med* 1989;30:1843-1847.

63. Iskandrian AS, Hakki AM. Thallium-201 myocardial scintigraphy. *Am Heart J* 1985;109:113-128.

64. Rozanski A, Berman DS, Gray R, et al. Use of thallium-201 redistribution scintigraphy in the preoperative differentiation of reversible and non-reversible myocardial asynergy. *Circulation* 1981;64:936-944.

65. Pohost GM, Zir LM, Moore RH, et al. Differentiation of transiently ischemic from infarcted myocardium by serial imaging after a single dose of thallium-201. *Circulation* 1977;55:294-302.

66. Berman DS, Garcia EV, Maddahi J, Rozanski A. Thallium-201 myocardial perfusion scintigraphy: redistribution. In: Freeman LM, ed. *Freeman & Johnson's clinical radionuclide imaging*, 3rd ed. Orlando: Grune & Stratton; 1984:481-82.

67. Kiat H, Berman D, Maddahi J, et al. Late reversibility of tomographic myocardial thallium-201 defects: an accurate marker of myocardial viability. *J Am Coll Cardiol*, Vol 12 No 6, 1456-63.

68. Gibson RS, Watson DD, Taylor GJ et al. Prospective assessment of regional myocardial perfusion before and after coronary revascularization surgery by quantitative thallium-201 scintigraphy. *J Am Coll Cardiol* 1983;1:804-815.

69. Brunken RC, Kotton S, Nienaber CA, et al. PET detection of viable tissue in myocardial segments were persistent defects at Tl-201 SPECT. *Radiology* 1989;172:65-73.

70. Schelbert HR, Buxton D. Insights into coronary artery disease gained from metabolic imaging. *Circulation* 78:496-505, 1988.

71. Marshall RC, Huang SC, Nash WW, et al. Assessment of the [<sup>18</sup>F]fluorodeoxy-glucose kinetic model in calculation of myocardial glucose metabolism during ischemia. *J Nucl Med* 1983;24:1060-1064.

72. Marshall RL, Tillisch JH, Phelps ME, et al. Identification and differentiation of resting myocardial ischemia and infarction in man with positron computed tomography. <sup>18</sup>F-labeled flurodeoxyglucose and N-13 ammonia. *Circulation* 67, No. 4, 1983:766-778.

73. Brunken R, Schwager M, Grover-McKay M, Phelps ME, Tillisch J, Schelbert HR. Positron emission tomography detects tissue metabolic activity in myocardial segments with persistent thallium perfusion defects. *J Am Coll Cardiol* 1987;10:557-567.

74. Brunken R, Tillisch J, Schelbert, et al. Regional perfusion, glucose metabolism, and wall motion in patients with chronic electrocardiographic Q wave infarction: evidence for persistence of viable tissue in some infarct regions by PET. *Circulation* 1986;3:951-963.

75. Schwaiger M, Brunken R, Grover-McKay M, et al. Regional myocardial metabolism in patients with acute myocardial infarction assessed by positron emission tomography. *J Am Coll Cardiol* Vol 8, No 4, Oct 1986:800-8.

76. Tillisch J, Brunken R, Marshall R, Schwaiger M, Mandelkern M, Phelps ME, Schelbert H. Reversibility of cardiac wall-motion abnormalities predicted by positron tomography. *N Engl J Med* 1986;314:884-888.

77. Tamaki N, Yonekura Y, Yamashita K, et al. Positron emission tomography using fluorine-18 deoxyglucose in evaluation of coronary artery bypass grafting. *Am J Cardiol* 1989;64:869-875.

78. Vaghaiwalla Mody F, Brunken RC, Nienaber CA, et al. Characterization of dilated and ischemic cardiomyopathy utilizing visual and circumferential profile analysis with PET [Abstract]. *J Nucl Med* 1988;29:818.

79. Brown M, Myears D, Bergmann S. Non-invasive assessment

of canine myocardial oxidative metabolism with carbon-11 acetate and positron emission tomography. *J Am Coll Cardiol* 1988;12:1054.

80. Brown M, Marshall DR, Sobel BE, Bergman S. Delineation of myocardial oxygen utilization with C-11-labeled acetate. *Circulation* 1987;76:687-696.

81. Bergmann SR, Brown MA. Validity of estimates of myocardial oxygen consumption using Carbon-11-acetate and positron emission tomography [Abstract]. *Circulation* 1988;78(suppl 11):11-322.

82. Armbrecht J, Buxton DB, Brunken RC et al. Noninvasive determination of regional myocardial oxygen metabolism in humans with C-11 Acetate and PET (abstract). *Circulation* 1988;78(4) Suppl II-599.

83. Walsh MN, Brown MA, Henes CG, et al. Estimation of regional myocardial oxidative metabolism by PET with carbon-11 acetate in patients (abstract). *Circulation* 1988;78 (4) Suppl II-599.

84. Armbrecht J, Buxton D, Brunken R, Phelps M, Schelbert H. Regional myocardial oxygen consumption determined non-invasively in humans with [ $^{11}\text{C}$ ] acetate and dynamic positron tomography. *Circulation* 1989;80(4):863-872.

85. Brown MA, Walsh MN, et al. Assessment of regional oxidative metabolism by PET with C-11 acetate in patients with myocardial infarction [Abstract]. *J Nucl Med* 1988;29:818.

86. Henes CG, Bergman SR, Walsh MN, Geltman EM. Recovery of myocardial perfusion and oxygen consumption after thrombolysis delineated with positron emission tomography (PET) [Abstract]. *Circulation* Supplement II; Vol 80, No. 4, 312 October 1989.

87. Rosamond TL, Abendschein DR, Sobel BE, et al. Metabolic fate of radiolabeled palmitate in ischemic canine myocardium: implications for positron emission tomography. *J Nucl Med* 1987;28:1322-1329.

88. Martins JB. Autonomic control of ventricular tachycardia: Sympathetic neural influence of spontaneous tachycardia 24 hours after coronary occlusion. *Circulation* 1985;72:933-942.

89. Inoue H, Zipes DP. Results of sympathetic denervation in canine heart: Supersensitivity that may be arrhythmogenic. *Circulation* 1989;75:877-887.

90. Eisen HJ, Nader RG, Reilly J, et al. Assessment of regional

myocardial adrenergic activity following myocardial infarction using I-123 metaiodobenzylguanidine [Abstract]. *Circulation* 1989;80:II-515.

91. Dae M, Herre J, Botvinick E, et al. Scintigraphic detection of denervated myocardium after infarction [Abstract]. *J Nucl Med* 1986;27:949.

92. Henderson EB, Kahn JK, Corbett R Jr, et al. Abnormal I-123 metaiodobenzylguanidine myocardial washout and distribution may reflect myocardial adrenergic derangement in patients with congestive cardiomyopathy. *Circulation* 1988;78:1192-1199.

93. Schofer J, Spielman R, Schuchert A, Weber I. Meta (123) iodobenzylguanidine (MIBG) scintigraphy in idiopathic dilated cardiomyopathy: a noninvasive method to assess catecholamine depletion [Abstract]. *Circulation* 1987;76:IV-308.

94. Hutchins GD, Rothey JM, Wieland DM, et al. Evaluation of G-[F-18] fluorometaraminol (FMR) kinetics in canine myocardium using PET. *J Nucl Med* 1988;29:807.

95. Schwaiger M, Kalff V, Rosenspire K, et al. Noninvasive evaluation of cardiac sympathetic nervous system by PET using the new catecholamine analogue C-11 HED in the human heart [Abstract]. *Circulation* 1989;80:II-515.

96. Law MP, Burgin J. Evaluation of CGP-12177 for characterization of Beta-adrenergic receptors by PET: In vivo studies in rat [Abstract]. *J Nucl Med* 1989;30:766-767.

97. Syrota A, Comar D, Paillot G, et al. Muscarinic cholinergic receptors in the human heart evidenced under physiological condition, by positron emission tomography. *Proc Natl Acad Sci* 1985;82:584-588.

98. Mullholland K, Kalff V, Hutchins G, et al. Myocardial kinetics of a new muscarinic receptor ligand: C-11 tropanyl benzilate methiodide (MTRB) [Abstract]. *Circulation* 1989;80:II-638.

99. Shelton ME, Dence CS, Huang DR, et al. Myocardial kinetics of fluorine-18 misonidazole: A marker of hypoxic myocardium. *J Nucl Med* 1989;30:351-358.

100. Shelton ME, Dence CS, Hwang DR, Welch MG, Bergmann SR. Enhanced extraction of [F-18] fluoromisonidazole by jeopardized myocardium assessed with PET [Abstract]. *J Nucl Med* 1989;30:730.